Preventive Control of Voltage Security Margins: A Multicontingency Sensitivity-Based Approach

Florin Capitanescu and Thierry Van Cutsem, *Member, IEEE*

***Abstract*—This paper addresses the problem of changing the operating point of a power system in order to keep voltage security margins with respect to contingencies above some minimal value. Margins take on the form of maximum pre-contingency power transfers either between a generation and a load area or between two generation areas. They are determined by means of a fast time-domain method. We will first discuss the use of a general optimal power flow, in which linear voltage security constraints are added. The simultaneous control of several (possibly conflicting) contingencies is considered. Then, we will focus on the minimal control change objective. Among the possible controls, emphasis is put on generation rescheduling and load curtailment. Examples are presented on an 80-bus test system as well as on a real system.**

***Index Terms*—Dynamic security analysis, generation rescheduling, load curtailment, preventive control, voltage stability.**

I. Introduction

VOLTAGE stability is a major aspect of power system security analysis in both operational planning and real-time [1], [2]. Voltage security analysis has become even more important in the open-access environment that prevails in an increasing number of power systems. In this context, it is the role of the transmission system operator to check security before a set of transactions is accepted, and to take preventive actions as soon as the security margins are deemed insufficient.

This paper is devoted to the determination of the best control actions to restore security margins with respect to credible contingencies.

Among the available controls, actions on voltages—through transformer ratios, generator voltages, and reactive power injections—are limited by the range of variation allowed for these variables as well as by the risk of pre-contingency overvoltages. On the other hand, active power generation rescheduling and load curtailment can have a significant impact on voltage stability. However, these actions have a cost and hence must be taken in a transparent and optimal manner.

Several publications deal with optimization techniques for preventive control of voltage stability. The various formulations aim at either maximizing a load power margin [5]–[8] or minimizing an objective function with voltage security constraints [8]–[11]. The approach used in this paper belongs to the second category.

There are basically two approaches to the computation of controls aimed at increasing a security margin.

1) The first approach is to perform a single optimization providing both the improved margin and the corresponding controls. Control and dependent variables are handled together. This optimization is performed with at least a set of equality constraints describing system operation at the limit point [5]–[7]. Inequality constraints can be added on the limit point [7] or on both the limit and the base case operating points [8], [11], which requires to incorporate the equality constraints relative to base case system operation.
2) The second approach is to import into an optimization of the base case system operation constraints stemming from a separate margin computation and analysis [9], [10].

Although it requires iteration between margin calculation and control adjustments, Approach B is more "open": e.g., margins can be determined through more accurate, dynamic simulations, while Approach A relies on algebraic (typically load flow) equations treated as equality constraints. In this paper, Approach B is followed, with the fast time-domain quasi-steady-state (QSS) simulation method [2] used to evaluate the system response to contingencies.

To the authors' knowledge, all publications so far concentrate on a single configuration of the system and, where a contingency is mentioned, the control actions are taken in the post-contingency configuration. Our concern is to control the system in the pre-contingency configuration such that security margins are maintained with respect to several (dangerous or potentially dangerous) contingencies simultaneously. In particular, we take into account that controls with positive effects on a contingency may be detrimental to another. Again, Approach B seems more appropriate, in as much as the multiple contingencies can be handled separately (and possibly in parallel), thereby breaking down the problem into more tractable ones.

II. Voltage Security Margins

Our analysis of voltage security relies upon the definition of a system stress. The latter consists of changes in bus power injections which make the system weaker by increasing power transfer over relatively long distances and/or drawing on reactive power reserves. Namely, at the ith bus, the load active power P_{li}, the load reactive power Q_{li}, or the generator active power P_{gi} vary according to

$$P_{li} = P_{li}^o + \lambda_{li} S \quad Q_{li} = Q_{li}^o + \mu_{li} S \quad P_{gi} = P_{gi}^o + \lambda_{gi} S$$

where

P_{li}^o, Q_{li}^o, and P_{gi}^o	corresponding base case values;
S	scaling factor;
$(\lambda_{li}, \mu_{li}, \text{and } \lambda_{gi})$	participation factors.

Manuscript received June 6, 2001; revised October 18, 2001.

The authors are with the Department of Electrical Engineering and Computer Science (Montefiore Institute), University of Liège, B-4000 Liège, Belgium (e-mail: t.vancutsem@ulg.ac.be).

Publisher Item Identifier S 0885-8950(02)03821-X.

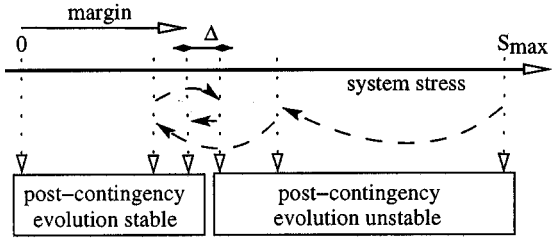

Fig. 1. Binary search of a security margin.

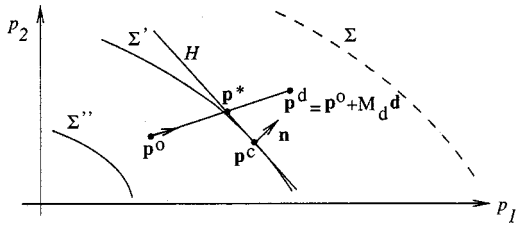

Fig. 2. Power injection space.

These equations can be written in vector form as

$$\mathbf{p} = \mathbf{p}^o + S\mathbf{d} \tag{1}$$

where

$\mathbf{p}$ vector of bus injections;
$\mathbf{p}^o$ base case value;
$\mathbf{d}$ vector defining the "direction of stress."

Typical stresses consist of increasing load in an area A and generation in a remote area B ($\lambda_{li}, \mu_{li} > 0, i \in A; \lambda_{gj} > 0, j \in B$) or decreasing generation in an area A and increasing generation in a remote area B ($\lambda_{gi} < 0, i \in A; \lambda_{gj} > 0, j \in B$).

For a given direction of stress, the margin M relative to a contingency is the maximum value of S such that the system can withstand this contingency [2]. Such a margin refers to pre-contingency parameters that operators can either observe or control.

The margin relative to a contingency can be determined by the simple and robust binary search. This consists of building a smaller and smaller interval $[S_\ell\ S_u]$, where S_ℓ corresponds to a stable post-contingency evolution and S_u to an unstable one, until $S_u - S_\ell$ becomes lower than a tolerance Δ. The search starts with $S_\ell = 0$ and $S_u = S_{\max}$, a maximum stress of interest. At each step, the interval is divided in two equal parts; if the midpoint is found stable (respectively, unstable) it is taken as the new lower (respectively, upper) bound. The final value of S_ℓ is the sought margin M. The procedure is sketched in Fig. 1, where the dashed arrows show the sequence of tested stress levels. It will be briefly illustrated in Section III-B.

In real-time applications, it is essential to filter out the contingencies and quickly identify those having low margins for the stress under concern. To this purpose, contingencies can be simulated on the system stressed at level $S_{\max}$, using a simplified method such as a post-contingency load flow. Contingencies which cause the latter to diverge or some voltages to drop by more than some amount are labeled potentially dangerous and are processed through the binary search using QSS simulation. Among them, the false alarms are discarded at the first step of the search.

Detailed examples and computing times relative to two real systems can be found in [4].

III. Linearized Voltage Security Constraints

A system is voltage secure when, for a specified direction of stress $\mathbf{d}$, the margin M relative to any of the specified contingencies is larger than some threshold M_d. Preventive voltage security control aims at modifying the pre-contingency operating point so that this constraint is met. In the sequel, we choose the control variables among the injection vector $\mathbf{p}^o$ (although the derivation could be extended to other controls as well).

Clearly, an essential information needed for control is the sensitivity of the margins to $\mathbf{p}^o$.

A. Derivation of Voltage Security Constraints

A simple, brute force approach consists in approximating the sensitivities by a ratio of finite differences, assuming a small variation Δp_j and evaluating the resulting margin variation ΔM. To guarantee accuracy, the magnitude of Δp_j must be chosen properly and the margins must be computed with a tolerance Δ smaller than what is needed for security monitoring. This requires to perform more steps in the binary search. On the other hand, each binary search can start from a narrower interval $[S_\ell\ S_u]$.

Deriving an accurate analytical expression of the sensitivities is a challenging—if at all solvable—problem. Indeed, we seek to determine how far changes in the *pre*-contingency operating point influence the maximum stress that can be imposed to the system, such that its response to a contingency is stable. A contribution of this paper is to show that the technique used in [12] for post-contingency control provides reasonably accurate information for the sought pre-contingency application.

The derivation is obtained as follows [2], [5], [12], [13].

The most common voltage instability mechanism is the loss of a long-term equilibrium. A two-dimensional view of the (parameter) space of power injections is given in Fig. 2. $\mathbf{p}^o$ corresponds to the base case demand, while $\mathbf{p}^d = \mathbf{p}^o + M_d\mathbf{d}$ corresponds to the desired margin. Under the effect of a contingency, the feasible region—where the system has a long-term equilibrium—shrinks, and its boundary changes from Σ to Σ'. $\mathbf{p}^d$ falls outside the new feasible region, and instability results. For the more severe contingency changing Σ to Σ'', the base case point $\mathbf{p}^o$ itself falls outside the new feasible region, which means that the system has no margin with respect to this contingency.

Preventive control aims at changing $\mathbf{p}^o$ into $\mathbf{p}^o + \Delta\mathbf{p}$ so that $\mathbf{p}^o + \Delta\mathbf{p} + M_d\mathbf{d}$ falls within the feasible region.

At this point, we use a linear approximation of the boundary surfaces, i.e., in Fig. 2 we approximate Σ' by its tangent hyperplane H. The latter is identified from the "critical point" $\mathbf{p}^c$ and the normal vector $\mathbf{n}$, whose computation will be explained in the sequel. In order $\mathbf{p}^o + \Delta\mathbf{p} + M_d\mathbf{d}$ to be brought back on the feasible side of H, $\Delta\mathbf{p}$ must satisfy

$$\mathbf{n}^T(\mathbf{p}^o + \Delta\mathbf{p} + M_d\mathbf{d} - \mathbf{p}^c) \leq 0 \Leftrightarrow -\mathbf{n}^T\Delta\mathbf{p} \geq \mathbf{n}^T(\mathbf{p}^o + M_d\mathbf{d} - \mathbf{p}^c). \tag{2}$$

An equivalent condition is derived as follows. Consider the point $\mathbf{p}^*$ in Fig. 2, corresponding to the margin $M(\mathbf{p}^o)$ before control. We have

$$\begin{aligned}\mathbf{n}^T(\mathbf{p}^o + M_d\mathbf{d} - \mathbf{p}^c) &= \mathbf{n}^T(\mathbf{p}^o + M_d\mathbf{d} - \mathbf{p}^* + \mathbf{p}^* - \mathbf{p}^c)\\ &= \mathbf{n}^T(\mathbf{p}^o + M_d\mathbf{d} - \mathbf{p}^*)\\ &= (\mathbf{n}^T\mathbf{d})(M_d - M(\mathbf{p}^o)).\end{aligned}$$

Introducing this result in (2) yields

$$M(\mathbf{p}^o) - \frac{\mathbf{n}^T}{\mathbf{n}^T\mathbf{d}}\Delta\mathbf{p} \geq M_d. \tag{3}$$

The row vector premultiplying $\Delta\mathbf{p}$ is the sensitivity of the margin to $\mathbf{p}^o$ and (3) expresses that the linear approximation of the post-control margin should be larger than M_d.

Denoting the set of long-term equilibrium equations by

$$\mathbf{g}(\mathbf{x}, \mathbf{p}) = \mathbf{g}(\mathbf{x}, \mathbf{p}^o + S\,\mathbf{d}) = \mathbf{0} \tag{4}$$

where $\mathbf{x}$ is the state vector; the normal vector is given by

$$\mathbf{n} = \mathbf{g}_\mathbf{p}^T\mathbf{w} \tag{5}$$

in which $\mathbf{g}_\mathbf{p}$ is the Jacobian of $\mathbf{g}$ with respect to $\mathbf{p}$ and $\mathbf{w}$ is the left eigenvector relative to the zero eigenvalue of the Jacobian $\mathbf{g}_\mathbf{x}$ on the bifurcation surface Σ' [2], [13].

Note that $\mathbf{w}$ is computed at a point where some generators may have switched under field current limit while they control their voltages in the base case. The voltage set points of such generators cannot be taken as control variables, since they do no longer appear in the final set of equations.

B. Illustrative Example

We consider the 80-bus system shown in Fig. 3, a variant of the "Nordic 32" system used, for example, by CIGRE Task Force 32.02.08 on long-term dynamics (1995). A rather heavy power transfer takes place from "north" to "south" areas.

The QSS long-term simulation reproduces the dynamics of load tap changers and overexcitation limiters. Note that there is no slack-bus in the QSS model; instead, generators respond to a disturbance according to governor effects [2]. Moreover, it is assumed that only the generators of the north area participate to frequency control (i.e., the others have infinite speed droops).

The stress of concern is a load increase in the south area ($S_{\max} = 600$ MW/180 MVAr)) covered by a generation increase in the north area ($S_{\max} = 630$ MW, accounting for losses), each according to participation factors.

We consider a set of 49 contingencies, out of which 20 have a margin lower than $S_{\max}$. Taking $\Delta = 50$ MW, five QSS simulations are needed to find a limit. The left plot in Fig. 4 shows the time evolution of a 400-kV bus voltage, under the effect of a contingency applied at $t = 10$ s. The curves relate to $S = 0, S_\ell, S_u$, and $S_{\max}$, respectively.

For each contingency of interest, the instability mode is identified from the marginally unstable case, using the technique detailed in [2] and [12]. First, the critical point is identified using the sensitivities of the total reactive generation to each reactive load. The time evolution of such a sensitivity is shown in the right plot of Fig. 4, relative to the marginally unstable case. The

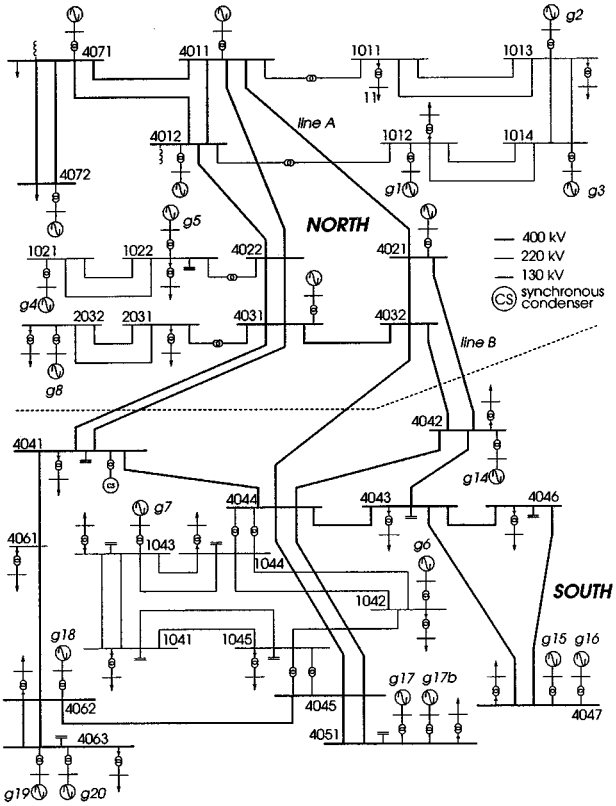

Fig. 3. Slightly modified "Nordic 32" test system.

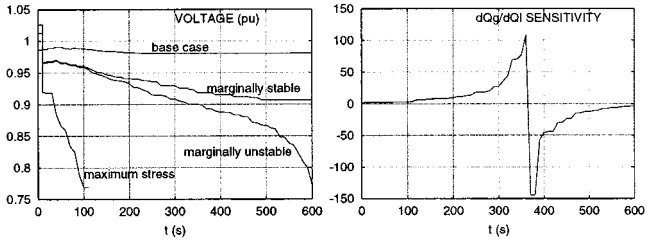

Fig. 4. Time evolution of a bus voltage and a $\partial Q_g/\partial Q_\ell$ sensitivity.

critical point is crossed at $t = 370$ s, where sensitivities change sign "going through infinity." At this point, the simultaneous iteration method applied to the Jacobian $\mathbf{g}_\mathbf{x}$ provides a small real positive dominant eigenvalue and the corresponding left eigenvector $\mathbf{w}$ to be substituted in (5).

Under the effect of field current limiters, the dominant (real) eigenvalue may "jump" from a negative to a positive value (e.g., [2, pp. 255–260]), instead of smoothly passing through zero. The above sensitivities correspondingly switch from positive to negative without assuming very large values, as in Fig. 4. As reported in [12], in all practical cases, we found it satisfactory to compute $\mathbf{w}$ at the first point where negative sensitivities are observed.

Table I shows the sensitivities of margins to controls given by (3), for the five most severe contingencies and for different controls. The sensitivity to an active generation is the margin increase for a small increase on this generation, balanced by a decrease of northern generations, as dictated by frequency control. Such values are presented in the first four rows of Table I. The last two rows, on the other hand, correspond to a shift of

TABLE I
NORDIC 32 SYSTEM: SENSITIVITIES GIVEN BY (3)

control :		contingency : loss of				
gener.	balanced by	g14	g17	line A	g15	g8
g17b	North	0.84	0.91	0.93	0.84	0.91
g18	North	0.80	0.84	0.92	0.80	0.88
g4	North	-0.09	-0.07	-0.12	-0.09	-0.09
g1	North	-0.02	0.00	-0.09	-0.02	-0.02
g17b	g4	0.93	0.98	1.05	0.93	1.00
g18	g1	0.82	0.84	1.01	0.82	0.90

TABLE II
SAME SYSTEM: SENSITIVITIES OBTAINED BY FINITE DIFFERENCES

control :		contingency : loss of				
gener.	balanced by	g14	g17	line A	g15	g8
g17b	North	0.86	1.04	0.98	0.96	0.92
g18	North	0.80	0.92	0.94	0.90	0.88
g4	North	-0.08	-0.16	-0.14	-0.10	-0.18
g1	North	0.00	-0.02	-0.22	-0.02	0.00
g17b	g4	0.94	1.10	1.08	1.02	1.02
g18	g1	0.82	0.92	1.00	0.90	0.88

power from one generator to another. The values have been obtained by subtracting the corresponding sensitivities.

Expectedly, these results show that margins are increased mainly by north to south power shifts, and much less by internal shifts within the north area.

For comparison purposes, Table II shows the same sensitivities obtained by finite differences. For each generator of concern, a 50-MW production increase has been considered, compensated according to governor effects. All margins have been computed with a Δ tolerance of 2 MW for the sake of accuracy.

Numerical discrepancies are to be expected considering that a finite difference is used, tap changers deadband make the QSS simulation somewhat insensitive, etc. Nevertheless, there is a good general agreement between both approaches. In particular, the ranking of control actions is the same by both approaches.

IV. OPTIMIZATION APPROACHES

Assume that system operation in the base case is characterized by c margins M_i smaller than the desired value M_d. The corresponding contingencies will be labeled as "harmful," the remaining ones being "harmless." We seek to modify $\mathbf{p}^o$ so that the c margins become at least as large as M_d. For each of them, (3) can be rewritten as

$$\sum_{j=1}^{n} S_{ij}\Delta p_j \geq M_d - M_i(\mathbf{p}^o) \quad i = 1, \ldots, c. \tag{6}$$

A. Control Provided by an Optimal Power Flow (OPF)

The inequalities (6) can be incorporated to the constraints of an OPF aimed at determining the n-dimensional vector $\Delta\mathbf{p}$ in some optimal manner.

In principle, this OPF can incorporate any other constraint, in particular, thermal limits relative to the base case and post-contingency configurations, thereby offering an integrated control of thermal and voltage problems.

Various OPF objectives can be considered. In a real-time environment, the insufficient margins represent transmission congestions, which should be corrected by adjusting the market-based generation scheme. Decomposing each correction into $\Delta p_j = \Delta p_j^+ - \Delta p_j^-$ with $\Delta p_j^+, \Delta p_j^- \geq 0$, a simple objective is

$$\min_{\Delta p_j^+, \Delta p_j^-} \sum_{j=1}^{n} \left(c_j^+ \Delta p_j^+ + c_j^- \Delta p_j^-\right) \tag{7}$$

where, for a generator which can be rescheduled, c_j^+ (respectively, c_j^-) is the incremental (respectively, decremental) bidding price, and for a load which can be curtailed, $\Delta p_j^+ = 0$ while c_j^- is the curtailment price.

Let $M_i(\mathbf{p}^o + \Delta\mathbf{p})$ $(i = 1, \ldots, c)$ be the new margins obtained after modifying $\mathbf{p}^o$ according to the OPF. We expect to have $M_i(\mathbf{p}^o + \Delta\mathbf{p}) \geq M_d$ $(i = 1, \ldots, c)$ with (at least) one inequality constraint (6) binding at the solution, i.e., $\exists k$: $M_k(\mathbf{p}^o + \Delta\mathbf{p}) = M_d$ or, in practice, $M_k(\mathbf{p}^o + \Delta\mathbf{p}) - M_d \leq \epsilon$, where ϵ is a tolerance. This corresponds to the most dangerous contingency in the post-control situation, with a margin just equal to M_d.

Two situations, however, may prevent us from reaching this objective in a single step, as discussed hereafter.

1) *Under- or over-correction of margins*. We have emphasized that the inequalities (6) are somewhat approximate with respect to the true nonlinear constraints. As a consequence, it can happen that some margins are still smaller than M_d or, on the contrary, all of them are significantly larger than M_d. In such cases, we compute improved sensitivities and redetermine the OPF correction to apply to $\mathbf{p}^o$ (not $\mathbf{p}^o + \Delta\mathbf{p}$!). Now, we only have c new margins to improve $cn \gg c$ sensitivities. To face this lack of information, we correct all the sensitivities S_{ij} $(j = 1, \ldots, n)$ relative to the ith contingency by the scaling factor

$$\frac{M_i(\mathbf{p}^o + \Delta\mathbf{p}) - M_i(\mathbf{p}^o)}{\sum_{j=1}^{n} S_{ij}\Delta p_j} \tag{8}$$

in which the numerator represents the real change in the ith margin and the denominator the one expected from linearization. This approximation is justified by the observation that, for a given contingency, the relative values of the various sensitivities S_{ij} are correct. In principle, the procedure has to be repeated until the margins are distributed as indicated previously.

2) *Antagonistic controls*. It can happen that changing $\mathbf{p}^o$ to meet the harmful contingency inequality constraints (6) causes harmless contingencies to become harmful. A first solution consists of extending the set of inequalities (6) to contingencies having a margin in an interval $[M_d\ M_d']$, where we assume that margins larger than M_d' (i.e., much larger than M_d) will not fall below M_d. Note that incorporating to the OPF more inequalities (6) than necessary has no consequence; the latter will merely remain nonbinding. Alternatively, we may stick with the M_d threshold and, if some new margins fall below M_d, add the corresponding inequalities to the former set and perform a new OPF.

Finally, we mention a variant that saves the initial margin computation. It consists of checking the contingencies after stressing the system at $\mathbf{p}^d = \mathbf{p}^o + M_d\mathbf{d}$. For the contingencies causing instability, (2) is used instead of (3), since $M(\mathbf{p}^o)$ is not known. The same technique is used, for the same reason, when a contingency causes instability in the base case. In practice, the identification of the critical point and eigenvector $\mathbf{w}$ from a very unstable trajectory may be more delicate than from a marginally unstable one.

B. Minimal Control Change: A Simplified Formulation

In the sequel, we focus on determining the minimal rescheduling and/or load curtailment needed to restore a certain level of voltage security. This is a particular case of the objective (7), corresponding to $c_j^- = c_j^+ = 1$, i.e., to

$$\min_{\Delta p_j^+, \Delta p_j^-} \sum_{j=1}^{n} \left(\Delta p_j^+ + \Delta p_j^-\right). \tag{9}$$

We ignore constraints on the pre-contingency operating point, and restrict our set of inequality constraints to

$$\sum_{j=1}^{n} S_{ij}\left(\Delta p_j^+ - \Delta p_j^-\right) \geq M_d - M_i(\mathbf{p}^o) i = 1, \ldots, c \tag{10}$$

$$0 \leq \Delta p_j^+ \leq p_j^{\max} - p_j^o$$
$$0 \leq \Delta p_j^- \leq p_j^o - p_j^{\min}. \tag{11}$$

Finally, we neglect the variations of network active losses and use instead the simple power balance equation

$$\sum_{j=1}^{n} \left(\Delta p_j^+ - \Delta p_j^-\right) = 0. \tag{12}$$

If this is not deemed acceptable, a full OPF incorporating (10) and (11) can be used (in which losses are taken into account through load flow equality constraints).

The above L_1-norm objective tends to put the control effort on generators with the highest sensitivities, even if the gap with respect to other generators is small. This drawback can be attenuated by limiting the amplitude of the control changes. An alternative is to use the L_2-norm objective

$$\min_{\Delta \mathbf{p}} \sum_{j=1}^{n} \Delta p_j^2. \tag{13}$$

The latter generally leads to a large number of injection changes, which can be impractical for transmission system operators. This disadvantage could be mitigated by performing a second optimization, after removing from the candidate controls, generators with small contributions Δp_j.

The above optimization problems can be solved using standard linear or quadratic programming software.

In the above formulation, controls are of active power nature, but reactive aspects can be accounted for in the computation of the sensitivities S_{ij}. More precisely, if a change in active power ΔP_j at the j-bus is accompanied by a change $\Delta Q_j = a_j \Delta P_j$ of the corresponding reactive power injection, the effective sensitivity is taken as

$$S_{ij} = \frac{\partial M_i}{\partial P_j} + a_j \frac{\partial M_i}{\partial Q_j}. \tag{14}$$

This formula is applied in the following two cases.

Load curtailment. When load is cut, both active and reactive powers vary. In the absence of a more precise information, loads can be decreased under constant power factor, in which case $a_j = Q_j^o / P_j^o$.

Generation rescheduling. It is well known from the capability curves that increasing the active production of a generator decreases its reactive reserve. To account for this effect, a_j is taken as the (negative) slope of the $Q(P)$ curve. This applies only to generators under reactive power limit at the critical point where $\mathbf{w}$ is computed.

If the last term in (14) is large enough, when decreasing active power generation, the benefit of an increased reactive reserve may outweight the detrimental effect of importing active power from remote generators.

The whole computational procedure is sketched in Fig. 5, where the dashed lines correspond to the variant mentioned in the last paragraph of Section IV-A.

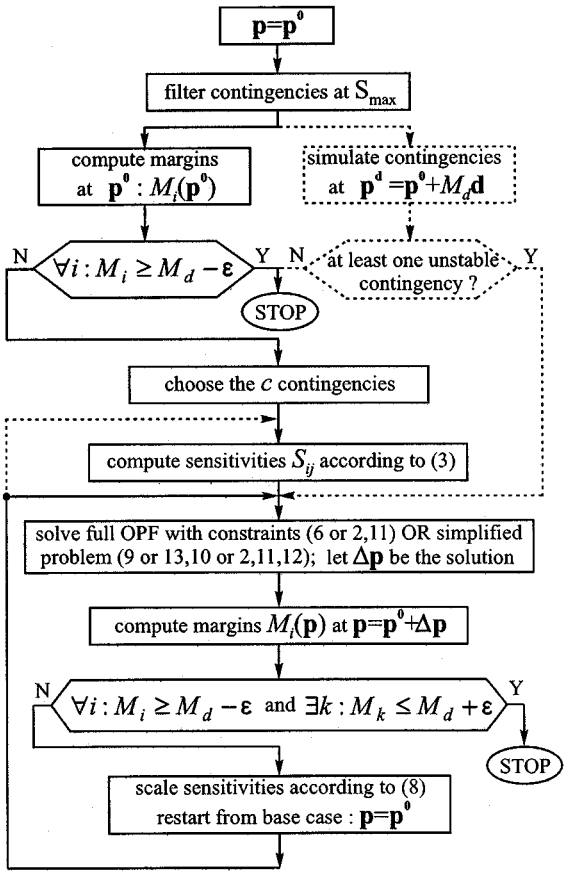

Fig. 5. Overall flowchart of the computational procedure.

C. Illustrative Example

We proceed with the example of Section III-B. For the same system stress, we request $M_d = 300$ MW. Ten contingencies

TABLE III
NORDIC 32 SYSTEM: MARGINS BEFORE AND AFTER CONTROL

contin-	security margins (MW)						
gency :	base	A	B		C	D	
loss of	case	it 1	it 1	it 2	it 1	it 1	it 2
g14	133	291	319	300	300	319	300
g17	180	366	347	328	338	356	338
g15	195	366	375	356	356	375	356
line A	195	375	375	356	384	384	356
g8	203	375	375	366	384	375	356
g16	234	394	413	394	384	413	394
g17b	281	338	459	450	450	469	450
g20	297	469	469	450	478	469	459
g18	297	478	469	450	459	488	469
g19	297	469	469	450	478	469	459
g6	344	525	525	506	497	534	516
line B	344	525	525	516	534	534	516

TABLE IV
NORDIC 32 SYSTEM: CHANGES IN GENERATION OR LOAD (IN MEGAWATTS)

gener.	A	B		C	D	
or load	it 1	it 1	it 2	it 1	it 1	it 2
g2				-45	-40	-36
g3				-45	-41	-37
g4	-178	-164	-147	-49	-45	-41
g5				-48	-44	-40
g6				26		
g7	43			31		
g15				25		
g16				25		
g17				28		
g17b	135			28		
g18				24		
1043					38	38
1044		-134	-134		45	40
1045		-30	-13		44	39
4042					43	37

are harmful, i.e., have a margin smaller than M_d, as shown in the second column of Table III. To anticipate for antagonistic effects, we choose $M'_d = 350$ MW. This leads to monitoring $c = 12$ contingencies.

We consider hereafter four combinations of controls and objectives, whose results are detailed in Tables III and IV.

Case A: L_1 norm, generation rescheduling. The optimization problem (9)–(11) leads to reschedule 178 MW (objective function (9)$= 178 \times 2 = 356$ MW). It consists of increasing the production of generators g7 and g17b which are located in the voltage sensitive area, while decreasing the generation of g4, located far away in the north. This decreases the north to south power transfer. Since after this generation shift, all margins are above 300 MW and one of them (loss of g14) approaches this threshold by less than $\epsilon = 10$ MW, there is no need for another optimization. We observe that the margin relative to the loss of generator g17b increases significantly less (57 MW) than the others (from 158 to 186 MW). This is due to the fact that rescheduling increases the production of g17b by 135 MW, and hence the loss of this increased generation causes the north to south transfer to increase correspondingly (due to already mentioned governor effects).

Case B: L_1 norm, load curtailment. In this second example, both generation rescheduling and load curtailment are allowed to restore security margins. The maximal interruptible fraction of each load is limited to 20% and power factors are preserved. The solution consists of shedding 147 MW in the voltage sensitive area, and again compensating on the remote generator g4. With respect to Case A, the objective function (9) reaches a lower value (294 MW) thanks to the larger number of controls offered. In this case, a second optimization is needed to make the smallest margin approach 300 MW by less than ϵ.

Case C: L_2 norm, generation rescheduling. This case is the same as Case A, except for the objective, which is taken as (13). This yields a larger number of changes, each of smaller magnitude. The changes have been, however, limited to 11 generators, selected on the basis of their sensitivities. The total rescheduling is 187 MW, i.e., somewhat more than that with the L_1 norm.

Case D: L_2 norm, load curtailment. Similarly, the effort is shared by a larger number of loads than in Case B.

As a general remark, the L_1 optimization yields a smaller number of changes and a smaller total power change. On the other hand, the L_2 optimization is more robust with respect to inaccuracies on the sensitivities that could lead to shifting the control effort from one generator to another.

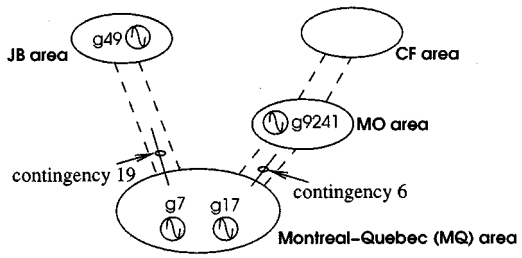

Fig. 6. Overall structure of the Hydro-Québec 735-kV system.

D. Example From the Hydro-Québec System

We briefly present here an example of antagonistic controls observed on the Hydro-Québec (HQ) system. Fig. 6 sketches the structure of the 735-kV transmission system. More details can be found in [4]. Let us only emphasize here that the system response is much influenced by the operation of an extended set of shunt reactor tripping devices. The long-term evolution of voltages is thus very dynamic by nature, which has motivated the adoption of QSS simulation by HQ engineers for security limit computations. Examples of the latter are given in [4].

The stress consists of increasing the demand in the Montreal-Québec (MQ) area, where most of the load is concentrated, and the generation in the JB, CF, and MO areas. Security limits are computed for a set of 37 contingencies, with $S_{\max} = 1000$ MW. Two contingencies have limits lower than $S_{\max}$ (see Table V). They are located in the MO–MQ and JB–MQ corridors, respectively.

We consider the minimal generation rescheduling in the L_1 sense, corresponding to four values of M_d. The computed controls are shown in Table VI. Three successive optimizations are required on the average. This is attributed to the fact that margins change more abruptly with controls, under the effect of shunt reactor trippings.

TABLE V
HYDRO-QUÉBEC SYSTEM: PRE-AND POST-CONTROL MARGINS

contingency	margins (MW) base case	after rescheduling, for M_d = 300	400	425	525
6	264	299	398	428	529
19	398	480	469	428	399

TABLE VI
HYDRO-QUÉBEC SYSTEM: GENERATION RESCHEDULING (IN MEGAWATTS)

gener	$M_d = 300$	$M_d = 400$	$M_d = 425$	$M_d = 525$
g9241	-35	-48	-67	-137
g7	27	27	27	27
g17	8	13	13	13
g49		8	27	97

For $M_d = 300$ MW, contingency 6 is harmful. Expectedly, the minimal generation rescheduling consists of decreasing the power flow in the MO–MQ corridor, shifting 35 MW from g9241 (MO area) to g7 and g17 (MQ area). Both margins are increased. However, after this preventive control, almost no active power reserve is left to the MQ area. Therefore, when M_d is set to 400 MW, the minimal generation rescheduling slightly increases the production of g49, located in the JB area. This is accompanied by a slight decrease in the margin of contingency 19 (which, however, remains above M_d). If M_d is set to 525 MW, for instance, the problem is infeasible. Indeed, at this level, bringing both margins above M_d would require to decrease both corridor flows. The largest value of M_d for which a solution exists is 425 MW. The corresponding results are given in Tables V and VI; both margins have been raised at the 425 MW threshold. By setting (for checking purposes) M_d to 525 MW for contingency 6 and 400 MW for contingency 19, the problem is feasible again, with the solution shown in the last column of each table.

V. CONCLUSION

This paper has dealt with the preventive control to restore margins at a desired level. Emphasis has been put on power injections as control variables.

Among the features of the proposed method, let us quote:

- the determination of sensitivities of pre-contingency margins to controls using post-contingency information;
- the derivation of linearized security constraints to be included in an OPF, possibly together with the similar constraints stemming from line overloads in a unified treatment of voltage and thermal security;
- a technique to compensate for the linear approximation (two OPF runs are generally sufficient to make the system secure without under- or over-correcting);
- the simultaneous control of all harmful contingencies;
- the handling of antagonistic controls by incorporating some harmless contingencies in the constraints.

Successful results have already been obtained when extending the techniques described in this paper to the modification of bilateral transactions (stemming, for instance, from external systems) instead of individual injections. A further extension is the modification of a market-based unit commitment to meet voltage security margins.

Regarding computational efforts, the optimization procedure by itself is a fast step of the overall procedure, especially if the simplified formulation of Section IV-B is used. The main effort lies in the (re)evaluation of margins. However, proven methods are now available to determine such margins [4]. Their coupling with appropriate filtering techniques and their implementation on modern (possibly distributed) computer hardware allow to envisage real-time applications.

REFERENCES

[1] C. W. Taylor, "EPRI power system engineering series," in *Power System Voltage Stability*. New York: McGraw-Hill, 1994.
[2] T. Van Cutsem and C. Vournas, *Voltage Stability of Electric Power Systems*. Norwell, MA: Kluwer, 1998.
[3] T. Van Cutsem, "Voltage instability: Phenomena, countermeasures, and analysis methods," *Proc. IEEE*, vol. 88, pp. 208–227, 2000.
[4] T. Van Cutsem, F. Capitanescu, C. Moors, D. Lefebvre, and V. Sermanson, "An advanced tool for preventive voltage security assessment," in *Proc. VII SEPOPE Conf.*, Curitiba, Brazil, 2000, Paper IP-035.
[5] I. Dobson and L. Lu, "Computing an optimum direction in control space to avoid saddle node bifurcation and voltage collapse in electric power systems," *IEEE Trans. Automat. Contr.*, vol. 37, pp. 1616–1620, Oct. 1998.
[6] C. A. Canizares, "Calculating optimal system parameters to maximize the distance to saddle-node bifurcations," *IEEE Trans. Circuits Syst. I*, vol. 45, pp. 225–237, 1998.
[7] R. Wang and R. H. Lasseter, "Re-dispatching generation to increase power system security margin and support low voltage bus," *IEEE Trans. Power Syst.*, vol. 15, pp. 496–501, May 2000.
[8] W. Rosehart, C. A. Canizares, and V. H. Quintana, "Optimal power flow incorporating voltage collapse constraints," in *Proc. IEEE PES Summer Meeting*, Edmonton, Canada, 1999, pp. 820–825.
[9] X. Wang, G. C. Ejebe, J. Tong, and J. G. Waight, "Preventive/corrective control for voltage stability using direct interior point method," *IEEE Trans. Power Syst.*, vol. 13, pp. 878–883, Aug. 1998.
[10] Z. Feng, V. Ajjarapu, and D. J. Maratukulam, "A comprehensive approach for preventive and corrective control to mitigate voltage collapse," *IEEE Trans. Power Syst.*, vol. 15, pp. 791–797, May 2000.
[11] E. Vaahedi, Y. Mansour, C. Fuchs, S. Granville, M. de Lujan Lastore, and H. Hamadanizadeh, "Dynamic security constrained optimal power flow/VaR planning," *IEEE Trans. Power Syst.*, vol. 16, pp. 38–43, Feb. 2001.
[12] C. Moors and T. Van Cutsem, "Determination of optimal load shedding against voltage instability," in *Proc. 13th PSCC*, Trondheim, Norway, 1999, pp. 993–1000.
[13] S. Greene, I. Dobson, and F. L. Alvarado, "Sensitivity of the loading margin to voltage collapse with respect to arbitrary parameters," *IEEE Trans. Power Syst.*, vol. 12, pp. 262– 272, Feb. 1997.

Florin Capitanescu received the B.S. and M.Sc. degrees in electrical power engineering from the University "Politehnica" of Bucharest, Bucharest, Romania, in 1997 and 1998, respectively, and the DEA degree from the University of Liège, Liège, Belgium, in 2000, where he is currently pursuing the Ph.D. degree in preventive aspects of voltage security.

Thierry Van Cutsem (M'94) received the electrical-mechanical engineering and the Ph.D. degrees from the University of Liège, Liège, Belgium, in 1979 and 1984, respectively.

Since 1980, he has been with the Belgian National Fund for Scientific Research (FNRS) of which he is now a Research Director. He is currently an Adjunct Professor at the University of Liège. His research interests are in power system dynamics, control and stability, numerical simulation, and security analysis, in particular, voltage stability and security.